

Analysis and synthesis of motion patterns using the projective plane

Cicero Mota, Michael Dorr, Ingo Stuke[†], and Erhardt Barth

Institute for Neuro- and Bioinformatics

[†]Institute for Signal Processing

University of Lübeck, Ratzeburger Allee 160, 23538 Lübeck, Germany

ABSTRACT

We first review theoretical results for the problem of estimating single and multiple transparent motions. For N motions we obtain a $M \times M$ generalized structure tensor \mathbf{J}_N with $M = 3$ for one, $M = 6$ for two, and $M = 10$ for three motions. The analysis of motion patterns is based on the ranks of \mathbf{J}_N and is thus not only conceptual but provides computable confidence measures for the different types of motions. To resolve the correspondence between the ranks of the tensors and the motion patterns, we introduce the projective plane as a new way of describing motion patterns. In the projective plane, intrinsically 2D spatial patterns (e.g. corners and line ends) that move correspond to points that represent the only admissible velocity, and 1D spatial patterns (e.g. straight edges) that move correspond to lines that represent, as a set of points, the set of admissible velocities. We then show a few examples for how the projective plane can be used to generate novel motion patterns and explain the perception of these patterns. We believe that our results will be useful for designing new stimuli for visual psychophysics and neuroscience and thereby contribute to the understanding of the dynamical properties of human vision.

1. INTRODUCTION

Transparent motions are additive or multiplicative superpositions of moving patterns and occur due to reflections, semi-transparencies, and occlusions. Many problems in computer vision rely on motion estimation, but standard motion models fail in case of transparent motions. In the case of see-through displays, a theory of overlaid motions is also relevant for vision science in the traditional domain of modeling perception with the scope of optimizing displays. The perception of transparent motions has been studied as such. As an early result, it has been reported that when the number of moving layers is increased beyond two, subjects are no longer able to perceive all the patterns simultaneously.^{1,2} An overview on the perception of transparency can be found in [3].

Several approaches for the estimation of motion vectors for the case of multiple transparent motions are known.⁴⁻⁷ The non-linear transparent-motions equations introduced by Shizawa and Mase⁴ have been solved for an arbitrary number of motions.⁸ However, the problem of motion estimation is always linked to the problem of motion detection. This is because the assumptions under which the motion parameters can be estimated correctly are rarely fulfilled in real dynamic scenes. Therefore, a correct decision on what local or global motion model to use is often more important and difficult to obtain than the estimation of the motion parameters. As we shall see, the strength of our approach lies not only in providing new solutions for the motion parameters, but also confidence measures for different classes of motion patterns.

The purpose of our paper can be understood by analogy with the case of only one motion. Obviously, in case of no image structure, no motion can be determined. In case of 1D spatial structure (e.g. straight edges) the motion is still not defined. This is known as the aperture problem and is either solved by not estimating motion at 1D patterns or, in most cases, by estimating only a component of the motion vector that is orthogonal to the orientation of the 1D spatial pattern. For more than one motion, we encounter many more situations that are similar to the aperture problem in the sense that not all motion parameters can be estimated. This generalized aperture problem is therefore more complex and has, to our knowledge, only be addressed briefly in [9, 10].

Please send correspondence to E. Barth, barth@inb.uni-luebeck.de, Institute for Neuro- and Bioinformatics, phone: +49 3909 483, fax: +49 3909 545, Ratzeburger Allee 160, 23538 Lübeck, Germany

	1D	1D+1D	1D+1D+1D	2D	2D+1D	2D+1D+1D	2D+2D	2D+2D+1D	2D+2D+2D
\mathbf{J}_1	1	2	3	2	3	3	3	3	3
\mathbf{J}_2	1	2	3	3	4	5	5	6	6
\mathbf{J}_3	1	2	3	4	5	6	7	8	9

Table 1. Different motion patterns (table columns) and the ranks of the generalized structure tensors for 1, 2, and 3 motions (table rows). The intrinsic dimension is equal to the rank of \mathbf{J}_1 . This table summarizes our results by showing the correspondence between the different motion patterns and the tensor-ranks that can, in turn, be used to estimate the confidence for a particular pattern, i.e. a proper motion model. Observe that the rank of \mathbf{J}_N induces a natural order of complexity for patterns consisting of N additive layers.

Motion selectivity is a key feature of biological visual processing and has been studied by recordings of neural responses and by psychophysical experiments. Human observers are able to see and distinguish multiple transparent motions. A special case is that of overlaid 1D motions, i.e., the case of moving straight patterns. Of particular interest is how human observers resolve the ambiguities that are inherent in these type of patterns¹¹ and how visual neurons respond to such patterns.¹² This paper provides a framework for the analysis of these motion patterns, such that, for example, the motion of two overlaid 1D patterns (e.g. two gratings) can be distinguished from the motion of one 2D pattern. These patterns remain equivalent within traditional theories of only one motion. To accomplish this, first we establish a correspondence between motion patterns and subsets of the projective plane. This is done such that 2D moving patterns correspond to points and 1D moving patterns correspond to lines of the projective plane. This correspondence is then used to show that different motion patterns correspond to different ranks of the generalized structure tensor \mathbf{J}_N , see Table 1.

The best way to understand the benefits of our approach is to use the interactive tool that we make available.¹³

2. THE GENERALIZED STRUCTURE TENSOR

Our approach is based on the framework for estimating multiple motions, as introduced in [8, 14], that we will briefly summarize here. Suppose that an image sequence f is the overlaid superposition of N image layers g_1, \dots, g_N moving with constant but different velocities $\mathbf{v}_1, \dots, \mathbf{v}_N$ respectively:

$$f(\mathbf{x}, t) = \sum_{n=1}^N g_n(\mathbf{x} - t\mathbf{v}_n) \quad (1)$$

The case of multiplicative overlaid motions can be reduced to the above additive superposition by taking the logarithm. The effect of multiplicative and additive superpositions can be observed by using our interactive tool.¹³ In such an ideal case, it is known⁸ that image intensity f and the velocities are constrained by

$$\sum_I f_I c_I = 0 \quad (2)$$

where $I = (i_1, \dots, i_N)$ is an ordered sequence with components in $\{x, y, t\}$, f_I represents the N th-order partial derivative of f with respect to the components of I , the mixed-motion parameters c_I are the symmetric function of the coordinates of $\mathbf{V}_n = \mathbf{v}_n + \mathbf{e}_t$, for $n = 1, \dots, N$, and \mathbf{e}_t is the time axis.

The generalized structure tensor is defined by

$$\mathbf{J}_N = \omega * [(f_I)(f_I)^T] \quad (3)$$

where ω is a convolution kernel. Given the above constraints, the vector $c_N = (c_I)$, i.e. the vector with the mixed-motion parameters as its components, is a null eigenvector of J_N and can be estimated as the eigenvector associated to the smallest eigenvalue. The velocities are recovered from c_N by using the analytical method described in [8]. Obviously, the mixed-motion parameters can be computed only if the null eigenvalue is non-degenerated. For a single motion, the degeneracy of the null eigenvalue of J_1 is known to be equivalent to the aperture problem. In what follows, we will show that *generalized aperture problems* are equivalent to the degeneracy of the eigenvalues of J_N and are thus reflected in the ranks of J_N , see Table 1.

3. THE PROJECTIVE PLANE

Table 1 is useful for categorizing basic properties of multidimensional signals. Since motion patterns are of particular interest for vision science, it is important to obtain an intuitive understanding of such patterns. Traditionally, intuition and models have been improved by looking at Fourier correspondences. Thereby motion could be visualized as a plane in the transform domain and multiple motions there correspond to multiple planes. More specifically, the motion of a plaid is said to be determined by the two lines in the transform domain (that correspond to the two moving gratings), and because these two lines define a plane, the motion corresponding to that plane will be computed by algorithms and experienced by vision. However, this plane is not the only way to fit the two lines. It is known that different neurons encode this motion pattern differently and that the percept can vary depending on the energy distribution along the lines, e.g. it depends on the spatial frequency of the 1D patterns. For more than two motions, it becomes even harder to understand what overall motions would result from the superpositions of different moving patterns. We therefore introduce the projective plane as a mean of better describing overlaid motions.

The projective plane is obtained intuitively by adding to each line of the Euclidean plane an extra point called an *ideal point* and imposing that parallel lines share the same ideal point. The set of ideal points is called the ideal line. The intuitive concept can be made precise by use of homogeneous coordinates, i.e., each point of the projective plane is represented by a non-zero vector $P = (X, Y, Z)$. To make the representation unique it is imposed that P and Q represent the same point if $P = \lambda Q$. Points with a non-null Z -coordinate correspond to points of the Euclidean plane by the projection

$$x = X/Z, \quad y = Y/Z \quad (4)$$

while points with a null Z -coordinate represent the ideal points of the projective plane. By means of the above projection, a point (x, y) of the Euclidean plane becomes $(x, y, 1)$ in the projective plane.

Some properties of the projective plane are useful for the analysis and synthesis of motion patterns. They can be understood from the Cartesian representation of a projective line $\ell = \{(X, Y, Z); AX + BY + CZ = 0\}$. We summarize the main properties below:

- Duality: a line ℓ of equation $AX + BY + CZ = 0$ is associated to the point $V = (A, B, C)$ in the projective plane and vice-versa;
- Dimension reduction: lines and points of the projective plane correspond to planes and lines through the origin of the three-dimensional space respectively;
- No parallelism: any two lines of the projective plane do intersect;
- Two projective lines intersect at an ideal point if and only if their dual points and e_t are aligned in the projective plane.

Next we will apply these properties to the analysis and synthesis of motions patterns.

3.1. Analysis of multiple motions using the projective plane

A single pattern under rigid motion is described by

$$f(\mathbf{x}, t) = g(\mathbf{x} - t\mathbf{v}) \quad (5)$$

where \mathbf{v} is the velocity of the pattern. In the Fourier domain it becomes

$$F(\boldsymbol{\xi}, \xi_t) = \delta(\mathbf{v} \cdot \boldsymbol{\xi} + \xi_t)G(\boldsymbol{\xi}) \quad (6)$$

meaning that F is restricted to a plane through the origin of the Fourier domain. The velocity of the pattern being encoded by the normal to this plane. Such a plane in the Fourier domain corresponds to a line in the projective plane. The dual point to this line is precisely the velocity of the grating. To make the above discussion precise we introduce the *projective representation* of f by

$$\mathcal{P}_f(\mathbf{P}) = \frac{1}{\|\mathbf{P}\|} \int |F(s\mathbf{P})| ds \quad (7)$$

where \mathbf{P} is a vector representing a point in the projective plane. The factor $1/\|\mathbf{P}\|$ makes \mathcal{P}_f well defined for projective points. i.e., $\mathcal{P}_f(\mathbf{P}) = \mathcal{P}_f(\mathbf{Q})$ if \mathbf{P} and \mathbf{Q} are parallel.

To illustrate the usefulness of the framework, we show how to geometrically determine the velocity of one 2D moving pattern: the moving pattern is mapped to a plane in the Fourier domain, where it is further projected onto the projective plane resulting in a modulated Dirac line. The velocity is picked by applying the duality, here denoted with \mathcal{D} , to the Dirac line. The process is schematically shown below:

$$\text{moving pattern} \xrightarrow{\mathcal{F}} \text{plane} \xrightarrow{\mathcal{P}} \text{line} \xrightarrow{\mathcal{D}} \text{velocity.}$$

In the case of a 1D-pattern, e.g. a spatial grating, that is, $g(\mathbf{x}) = \tilde{g}(\mathbf{a} \cdot \mathbf{x})$, its Fourier transform reduces to a line, and its projective transform to a point. The duality operation will give us the set of admissible velocities for the grating which is a line in the projective plane:

$$\text{moving grating} \xrightarrow{\mathcal{F}} \text{line} \xrightarrow{\mathcal{P}} \text{point} \xrightarrow{\mathcal{D}} \text{admissible velocities.}$$

We summarize the main points below:

- The projective representation of f is the superposition of Dirac lines in the projective plane (in case of 2D patterns);
- The dual point to each Dirac line in the projective plane is the velocity of the respective layer;
- For a 1D pattern, its Dirac line in the projective plane further reduces to a Dirac point. In this case any admissible velocity for the grating is a point of the line dual to the Dirac point in the projective plane;
- Dirac lines intersect at an ideal point if and only if their corresponding spatial velocities are collinear;
- A Dirac line supported by the ideal line corresponds to a static pattern.

As a further example, we show how to determine the *coherent motion* of superimposed gratings (plaids)¹¹: the set of admissible velocities for each layer is a line, the intersection of these two lines is the only admissible velocity for both layers, that is, the coherent velocity for the plaid. Further examples will be given in Section 4.

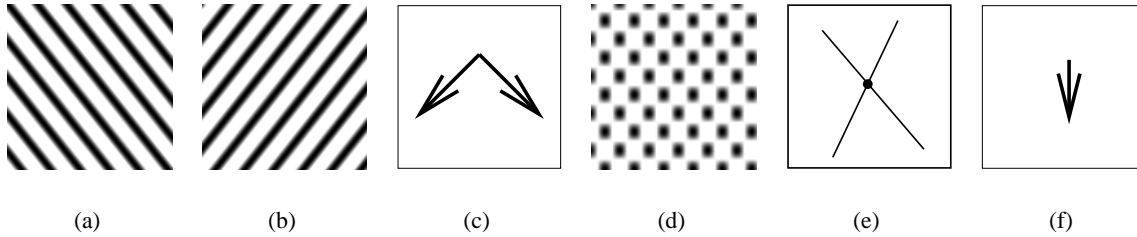


Figure 1. If two gratings of different orientations - as shown in (a) and (b) - are moved in the directions shown in (c), the plaid pattern shown in (d) is seen as moving in the direction indicated in (f) which corresponds to the only coherent velocity that is defined by the intersection of the lines as shown in (e).

3.2. Synthesis of multiple motions using the projective plane

For the synthesis of motion patterns we use the projective plane as the natural place for the selection of the admissible velocities. For sinusoidal gratings this works as follow: We select a line in the projective plane

$$AX + BY + CZ = 0 \quad (8)$$

by the choice of two points $P(p_x, p_y)$ and $Q(q_x, q_y)$. This gives

$$A = p_y - q_y, \quad B = q_x - p_x, \quad C = \begin{vmatrix} p_x & p_y \\ q_x & q_y \end{vmatrix}. \quad (9)$$

The point dual to this line, represented by (A, B, C) , encodes the support of the projective representation of the grating. Consequently, the sinusoidal grating is defined by

$$g(\mathbf{x}) = \sin 2\pi(Ax + By) \quad (10)$$

with frequency vector (A, B) . For any admissible velocity \mathbf{v} , the equation of the moving grating is

$$f(\mathbf{x}, t) = g(\mathbf{x} - \mathbf{v}t) = \sin 2\pi(Ax + By + Ct). \quad (11)$$

Note that a moving sinusoidal grating is just a convenient choice since it can be synthesized efficiently through the trigonometric identities for the sinus function.

In our interactive tool, 2D patterns are synthesized as moving noise patterns. Therefore, we use the projective plane simply for the selection of the desired velocity. In addition, the variance of the noise pattern can be adjusted.

3.3. The patterns in the projective plane and the rank of J_N

Up to now we have derived a correspondence between different motion patterns and subsets of the projective plane (points and lines). The problem of determining the rank of J_N is equivalent to the problem of finding the largest number of independent null-eigenvectors. This task becomes simpler when we look at the projective representation of f . We give the detail in the appendix. Table 1 summarizes the correspondence between motion patterns and the ranks of J_1 , J_2 and J_3 .

4. APPLICATIONS TO SOME PERCEPTUAL PHENOMENA

For the case of only one motion, the aperture problem has a high significance for the visual perception of motion.¹⁵ As argued before, the motion of a 1D pattern is ambiguous from a theoretical point of view, and so are the percepts in the sense that they depend on the motion of the so-called terminators, i.e. the ends of the 1D patterns.

Similar effects appear with superimposed gratings that can induce motion percepts that are different from the directions orthogonal to the individual gratings. For example, two gratings, one moving down and to the left, the other one

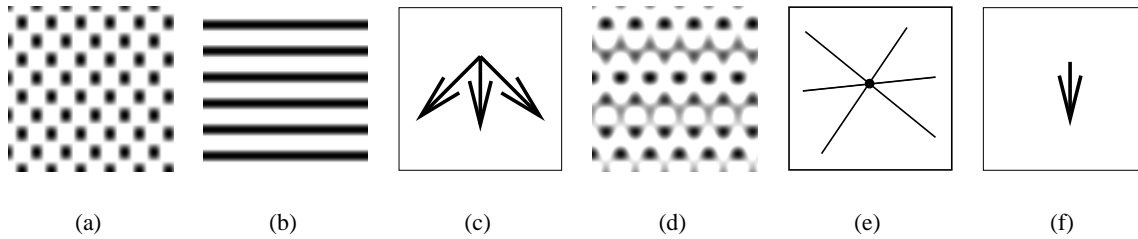


Figure 2. Coherent motion of three superimposed gratings. To the superposition of two gratings (a) a third grating shown in (b) is added. The physical motions of the three gratings are as shown in (c) and the lines of admissible velocities for each grating in (e). The percept is that of a coherent pattern as shown in (d) moving in the direction indicated by the arrow in (f). The coherent percept of one motion corresponds to the intersection of the lines in only one point.

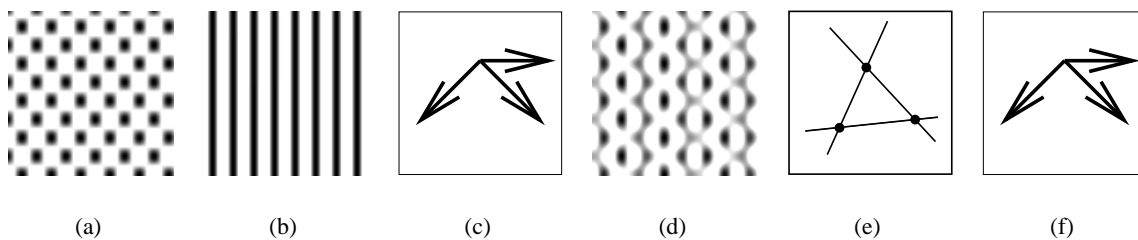


Figure 3. Incoherent motion of three superimposed gratings. The individual panels are according to those in Fig. 2. However, the directions of motions are now changed such that the lines of motion in the projective plane do not intersect in a single point (e). This makes the motions undefined and causes the percept to change dramatically such that a coherent motion is not perceived. Observers can see either of the single motions indicated in (f).

moving down and to the right, are perceived as a single pattern moving downwards under most experimental conditions - see Fig. 2. On the other hand, three moving gratings can give rise to three mutually exclusive percepts.¹¹ We are now going to explain these phenomena using our theoretical framework presented above. Before, we had used the framework to also predict a new illusion.¹⁰ In the projective plane, the admissible velocities for two moving gratings correspond to two lines. According to the theory, the perceived motion should correspond to the intersection point U of the two lines and indeed it does - see Fig. 1. In the case of three moving gratings, a percept of one coherent pattern only arises when all three lines intersect in the same point. This is, for example, the case for the configuration shown in Fig. 2. On the other hand, a configuration as shown in Fig. 3 has no unique percept: human observers see the three 1D patterns as moving individually or see combinations of one 1D pattern and a 2D plaid pattern.

5. DISCUSSION

We have presented a way of categorizing transparent-motion patterns in terms of the ranks of the generalized structure tensors. Based on these results, the confidence for a particular pattern can be evaluated computationally by either determining the rank J_N or by using the minors of the structure tensors.⁸ For example, we can discriminate the case of two superimposed 1D patterns (moving plaid) and a 2D pattern moving in the direction of the coherent motion of the plaid pattern.

Our results can be seen as an extension of the concept of *intrinsic dimension*.^{16,17} In the current framework, the intrinsic dimension corresponds to the rank of J_1 . As shown in Table 1, by introducing the generalized structure tensor, we can further differentiate the signal classes of a given (integer) intrinsic dimension. In some sense, we thereby define fractional intrinsic dimensions.

Although motion estimation is a key component of many computer-vision and image processing systems, the motion models are often too simple and fail with realistic data. Our results provide (i) new means for increasing the complexity of the motion models and (ii) measures for determining the confidence for a particular model. We should note that the

framework can be applied to make explicit the correspondence between the ranks of J_N , for an N larger than 3, and the different motion patterns.

We have also shown how our results can be used to describe some phenomena in biological vision. In particular, the concept of the projective representation of a motion pattern proved useful for describing and visualizing different visual percepts.

ACKNOWLEDGMENTS

Work is supported by the *Deutsche Forschungsgemeinschaft* under Ba 1176/7-2. We thank Martin Haker for implementing the interactive tool.¹³

REFERENCES

1. J. B. Mulligan, "Motion transparency is restricted to two planes," *Inv Ophth Vis Sci (suppl)* **33**, p. 1049, 1992.
2. J. B. Mulligan, "Nonlinear combination rules and the perception of visual motion transparency," *Vision Research* **33**(14), pp. 2021–30, 1993.
3. O. Braddick and N. Quian, "The organization of global motion and transparency," in *Motion Vision - Computational, Neural, and Ecological Constraints*, J. M. Zanker and J. Zeil, eds., pp. 86–111, Springer Verlag, Berlin Heidelberg New York, 2001.
4. M. Shizawa and K. Mase, "Simultaneous multiple optical flow estimation," in *IEEE Conf. Computer Vision and Pattern Recognition*, **I**, pp. 274–8, IEEE Computer Press, (Atlantic City, NJ), June 1990.
5. M. J. Black and P. Anandan, "The robust estimation of multiple motions: parametric and piecewise-smooth flow fields," *Computer Vision and Image Understanding* **63**, pp. 75–104, Jan. 1996.
6. T. Darrell and E. Simoncelli, "Nulling filters and the separation of transparent motions," in *IEEE Conf. Computer Vision and Pattern Recognition*, pp. 738–9, IEEE Computer Press, (New York), June 14–17, 1993.
7. W. Yu, K. Daniilidis, S. Beauchemin, and G. Sommer, "Detection and characterization of multiple motion points," in *IEEE Conf. Computer Vision and Pattern Recognition*, **I**, pp. 171–7, IEEE Computer Press, (Fort Collins, CO), June 23–25, 1999.
8. C. Mota, I. Stuke, and E. Barth, "Analytic solutions for multiple motions," in *Proc. IEEE Int. Conf. Image Processing*, **II**, pp. 917–20, IEEE Signal Processing Soc., (Thessaloniki, Greece), Oct. 7–10, 2001.
9. E. Barth, M. Dorr, I. Stuke, and C. Mota, "Theory and some data for up to four transparent motions.," *Perception* **30** (Supplement), p. 36, 2001.
10. C. Mota, M. Dorr, I. Stuke, and E. Barth, "Categorization of transparent-motion patterns using the projective plane," in *Proc. ACIS 4th Int. Conf. Software Engineering, Artificial Intelligence, Networking and Parallel/Distributed Computing*, W. Dosch and R. Y. Lee, eds., pp. 633–9, (Lübeck, Germany), Oct. 16–18, 2003.
11. E. H. Adelson and J. A. Movshon, "Phenomenal coherence of moving visual patterns," *Nature* **300**(5892), pp. 523–5, 1982.
12. J. A. Movshon, E. H. Adelson, M. Gizzi, and W. T. Newsome, "The analysis of moving visual patterns," in *Study group on pattern recognition mechanisms*, C. Chagas, R. Gattas, and C. G. Gross, eds., pp. 117–151, Pontifica Academia Scientiarum, Vatican City, 1985.
13. "An interactive tool for the synthesis of multiple motions by using the projective plane." <http://www.inb.uni-luebeck.de/vision/demos/ppmotion.html>, 2003.
14. E. Barth, I. Stuke, T. Aach, and C. Mota, "Spatio-temporal motion estimation for transparency and occlusion," in *Proc. IEEE Int. Conf. Image Processing*, **III**, pp. 69–72, IEEE Signal Processing Soc., (Barcelona, Spain), Sept. 14–17, 2003.
15. S. Wuerger, R. Shapley, and N. Rubin, "On the visually perceived direction of motion by Hans Wallach: 60 years later," *Perception* **25**, pp. 1317–67, 1996.
16. C. Zetsche and E. Barth, "Fundamental limits of linear filters in the visual processing of two-dimensional signals," *Vision Research* **30**, pp. 1111–7, 1990.
17. E. Barth and A. B. Watson, "A geometric framework for nonlinear visual coding," *Optics Express* **7**, pp. 155–85, 2000. <http://www.opticsexpress.org/oearchive/source/23045.htm>.

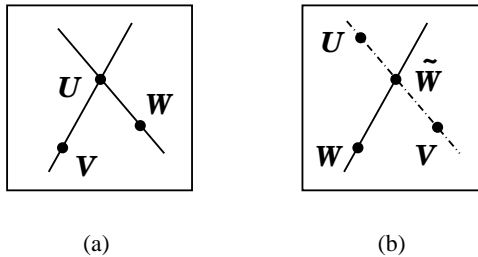


Figure 4. Admissible velocities of overlaid-motion patterns in the projective plane: (a) two overlaid 1D patterns, U is the coherent velocity, $c(\mathbf{u}, \mathbf{u}), c(\mathbf{u}, \mathbf{v}), c(\mathbf{u}, \mathbf{w}), c(\mathbf{v}, \mathbf{w})$ are independent null-eigenvectors of \mathbf{J}_2 ; (b) same for one 1D pattern and two 2D patterns, $c(\mathbf{u}, \mathbf{v}, \mathbf{w})$ and $c(\mathbf{u}, \mathbf{v}, \tilde{\mathbf{w}})$ are independent null-eigenvectors of \mathbf{J}_3 .

APPENDIX A. TRANSPARENT-MOTION PATTERNS AND THE RANK OF \mathbf{J}_N

From the discussion in Section 3.1, we have seen that the set of admissible velocities of a moving layer g is the dual space to the support of \mathcal{P}_G . This dual set is called the *phase space* for the velocities of g . In what follows, we will suppose that no pair of layers forming f moves with collinear velocities and none of the layers is static. This means that the lines supporting two non-degenerated Dirac lines always intersect at a finite (non-ideal) point.

The mixed-motion parameters vectors $\mathbf{c}_N = \mathbf{c}(\mathbf{v}_1, \dots, \mathbf{v}_N)$ can be interpreted as elements of the space of symmetric N -tensors (here denoted by \mathcal{S}_N). Therefore, if $\beta = \{\mathbf{U}, \mathbf{V}, \mathbf{W}\}$ is a basis for the three-dimensional Euclidean space, the set $\{\mathbf{c}(\mathbf{v}_1, \dots, \mathbf{v}_N) : \mathbf{V}_n \in \beta, \text{ for } n = 1, \dots, N\}$ is a basis for \mathcal{S}_N . For example, $\{c(\mathbf{u}, \mathbf{u}), c(\mathbf{u}, \mathbf{v}), c(\mathbf{u}, \mathbf{w}), c(\mathbf{v}, \mathbf{v}), c(\mathbf{v}, \mathbf{w}), c(\mathbf{w}, \mathbf{w})\}$ for \mathcal{S}_2 . We will use this relationship between basis of \mathbb{R}^3 and \mathcal{S}_N to construct a maximal number of elements in the kernel of \mathbf{J}_2 and \mathbf{J}_3 . By ‘kernel of \mathbf{J}_N ’ we denote the set of vectors that correspond to the zero eigenvalues of \mathbf{J}_N .

A.1. The rank of \mathbf{J}_2

For two moving layers, the non-trivial possibilities for the phase space of the velocities are a {line, line}, {point, line}, {point, point}. We will analyze the first case below and refer to [10] for further details. Choose a basis $\beta = \{\mathbf{U}, \mathbf{V}, \mathbf{W}\}$ of \mathbb{R}^3 such that U is intersection of the two lines, and V and W belong to each of these lines, see Fig. 4(a). Now it is clear that $c(\mathbf{u}, \mathbf{u}), c(\mathbf{u}, \mathbf{v}), c(\mathbf{u}, \mathbf{w})$ and $c(\mathbf{v}, \mathbf{w})$ are elements in the kernel of \mathbf{J}_2 . Since these vectors are linearly independent, we can conclude that $\text{rank}(\mathbf{J}_2) \leq 2$. Since it is possible to reach this bound, it is actually tight. Note that two moving patterns do not produce rank 1 or 3. These ranks are actually produced by a single moving object. The phase space for the two velocities, in this case, is {line, plane} or {point, plane}. We analyze the first case only, the other is similar: choose U, V as points in the line and W out of it. The only element that does not belong to the kernel of \mathbf{J}_2 is $c(\mathbf{w}, \mathbf{w})$ and therefore $\text{rank}(\mathbf{J}_2) = 1$.

A.2. The rank of \mathbf{J}_3

For three moving patterns, the non-trivial possibilities for the phase spaces of the velocities are a {line, line, line}, {point, line, line}, {point, point, line} and {point, point, point} which correspond to the values 3, 6, 8 and 9 of the rank of \mathbf{J}_3 . Since the analyses of these cases are very similar, we consider only one case. Choose U, V as the points and W in the line, see Fig. 4(b). In principle it appears that only the element $c(\mathbf{u}, \mathbf{v}, \mathbf{w})$ belongs to the kernel of \mathbf{J}_3 . To reveal another one, note that any two lines intersect in the projective plane. Let \tilde{W} be the intersection of the given line with the line determined by U and V . Now, if we assure that W does not coincide with \tilde{W} , we find the second independent symmetric tensor in the kernel of \mathbf{J}_3 , that is, $c(\mathbf{u}, \mathbf{v}, \tilde{\mathbf{w}})$. We conclude that $\text{rank}(\mathbf{J}_3) \leq 8$. Since these are all the possibilities, except maybe for degenerate cases, the bound 8 is tight.

Similar to the case \mathbf{J}_2 , three moving patterns do not fill all the possibilities for the rank of \mathbf{J}_3 . The gaps are filled by single or two moving patterns. These correspond to ranks 1,4 and 2,5,7 respectively. Table 1 summarizes the possibilities for the ranks of \mathbf{J}_N for $N = 1, 2, 3$.